 DOI: 10.31276/VJSTE.2024.0105

Effect of accelerated time-dependent corrosion on reinforcement concrete and ultra-high performance concrete: Finite element method analysis

Nguyen Thanh Hung[1], Duy Kien Dao[1*], Doan Dinh Thien Vuong[1], Le Quang Tang[2]

[1]*Department of Civil Engineering, Ho Chi Minh City University of Technology and Education, 1 Vo Van Ngan Street, Linh Chieu Ward, Thu Duc City, Ho Chi Minh City, Vietnam*
[2]*Department of Civil Engineering, Mien Trung University of Civil Engineering, 24 Nguyen Du Street, Tuy Hoa Ward, Dak Lak Province, Vietnam*

Received 4 October 2024; revised 11 November 2024; accepted 27 December 2024

Abstract:

In this study, finite element analysis using Ansys software was employed to evaluate the bond stress-slip behaviour of corroded steel bars in reinforced concrete structures. The corrosion specimen model was fabricated in accordance with the ACI 440.3R standard, comprising a 580-mm-long steel bar with diameters of 12, 16, and 20 mm, positioned at the centre of a 200x200x200 mm concrete block with varying compressive strengths of B25, B35, and B45, respectively. Following fabrication, the specimen was immersed in a tank containing a 3.5% NaCl saltwater solution. Subsequently, the electrochemical corrosion process, based on Faraday's law, was applied to accelerate corrosion. The concrete and steel bar elements were modelled using SOLID65 and LINK180, respectively. The elasto-plastic behaviour for both concrete and steel bars, along with the cohesive zone model (CZM) for the interface bond between the bar, whether corroded or not, and the concrete, demonstrated good agreement with experimental results. The experimental model was precisely constructed using Ansys software. The results obtained from finite element analysis exhibited high accuracy compared to the experiment, with a maximum error of only 4.5%. The finite element method (FEM) can entirely replace the experiment in analysing the adhesion force between concrete and steel. The constitutive models of materials could be applied for parametric studies in future work.

Keywords: **accelerated cyclic corrosion test, bond stress, corrosion levels, local corrosion, steel structure.**

Classification numbers: **2.1, 2.3, 5.3**

1. Introduction

After several years of service, reinforced concrete (RC) structures generally degrade for various reasons. One reason is that concrete deterioration allows water (H_2O), oxygen (O_2), or chloride ions (Cl^-) to penetrate through the cover thickness, causing corrosion of steel bars. Corrosion of the steel reinforcement bars reduces bond stress between the steel bars and surrounding concrete, diminishing the capacity of concrete structures. Therefore, the objective of this thesis is to investigate bond stress between steel bars and concrete under factors such as the diameter of the steel bar, compressive strength, and corrosion level.

Reinforced concrete has been widely utilised since the mid-19th century due to its flexibility, durability, and economy. During use, the current status of corrosion and deterioration of RC is a significant issue, especially in marine structures. Due to the characteristics of hot and humid climates with high ionic content, RC structures exhibit rust at varying levels, compromising the project's lifespan [1, 2]. Over a century of activity, the actual durability of RC works has been summarised globally as follows: in non-corrosive environments, RC structures can last sustainably for over 100 years; in aggressive marine environments, corrosion of reinforcement and concrete leading to cracking and destruction may appear after 10 to 30 years of use. The reliability of RC structures depends on environmental conditions and the quality of materials used (concrete strength, waterproofing, corrosion resistance, types of cement, additives, reinforcement type, design quality, construction, and management measures).

In fact, two main causes of reinforcement corrosion in RC structures are carbonation of concrete due to air ingress and ion penetration.

In the first case, air penetrates the concrete through a network of pores and fissures. In the presence of a liquid phase in concrete and cement hydration products, carbonation reactions occur, forming limestone. The pH of the medium decreases to approximately 9, resulting in the breakdown of the passive membrane that protects the reinforcement.

In the second case, ions penetrate the structure via the liquid phase, altering the protective environment of the

*Corresponding author: Email: kiendd@hcmute.edu.vn

concrete to the reinforcement, leading to changes in the passive membrane and promoting corrosion. Collected data shows the frequency and cost of building repairs due to corrosion [3].

In Vietnam, the effects of corrosion are even more pronounced compared to other countries due to high temperature, humidity, prolonged wet periods, and high chloride ion concentration. Many buildings are severely affected by corrosion after a short period. The current corrosion status of some structures in the North and South includes: (a) Cua Cam Port - Hai Phong, 25 km from the sea, after 30 years of use; (b) Trade Port - Vung Tau, after 15 years of use. Data show that structures are severely corroded up to 45%, with broken steel belts and peeled or broken protective concrete layers [4]. Many seaside construction sites built from the 1960s onwards have applied standard construction regulations, with little attention to corrosion protection requirements according to TCVN 9346:2012 standards [5].

When RC structures are in use, the adhesion between steel rebars and concrete is crucial. However, corrosion significantly reduces adhesion, leading to steel rebar slipping within the concrete. Consequently, the load-bearing capacity of the structure is rapidly reduced, causing structural failure. Accurately assessing the bond stress-slip behaviour between steel and concrete cannot be achieved during the design phase. The analysis of corroded RC structures has garnered significant attention from researchers worldwide, from experimental studies to finite element analysis and simulation.

P.V.D. Hoang, et al. (2017) [6] studied the bond stress-slip between geopolymer concrete (GPC) and reinforcement based on the pull-off test. Pull-off experiments were conducted for various reinforcement diameters and GPC grades. The length of the reinforced anchor section to the GPC is 10 cm. Experiments simulated in the ABAQUS environment investigated the bond between GPC and reinforcement, assuming no slip between them. Based on the match between simulation and experiment, the bond stress between GPC and reinforcement is shown to be quite good. Steel reinforcement will break when the anchor length is five times the steel diameter and the compressive strength of GPC is greater. Steel reinforcement will slip due to damage when the anchor length is five times the steel diameter and the compressive strength of GPC is less than or equal to 50MPa.

S. Lim, et al. (2016) [7] and M. Blomfors, et al. (2018) [8] studied the bonding model of corroded steel. They developed models to evaluate the anchoring ability of steel when corroded. This new model is based on the local bond-slip stress relationship from the Fib Model Code and has been adjusted for the corrosion mechanism. The results show significant inherent dispersion between experimental bonds, even in groups with the same corrosion degree. However, this new model can demonstrate a reasonable reduction in steel anchoring capacity, showing better experimental data than previous versions.

A.N. Kallias, et al. (2013) [9] studied the corrosion performance of flexible RC beams using the response surface method (RSM) and nonlinear finite element analysis (NLFEA) for validation. Corrosion effects are calculated using experimental/semi-experimental models based on experimental parameters. Low-order polynomial (RSM) models provided loads at the working limit deflection, flexural resistance, and behaviour coefficient (LD) of corrosion beams when using appropriate tests.

Z.H. Wang, et al. (2019) [10] studied the effect of ice on the bond between concrete and reinforcement using the Fibre model. The results show that the bonding efficiency of concrete and reinforcement is significantly reduced, with material degradation not uniform across concrete structure locations when affected by thawing and freezing.

W. Zhu, et al. (2013, 2014) [11, 12] evaluated the shape and tensile strength of corroded reinforcement through experiments. Mechanical property tests were conducted on eroded bars from RC beams exposed to chloride environments for 26 and 28 years. The study simulated three types of corrosion with different cross-section residual shapes, including homogeneous and heterogeneous sections, applied to non-corroded bars to study the effects of the remaining section shape on the final deformation of the steel bar. The results show that the remaining shape of the cross-section and the lost section significantly affect the tensile strength of the steel bars. For the same simulated corrosion level, the steel bar with the remaining symmetrical cross-section provides the best tensile strength.

J.G. Dai, et al. (2013) [13] studied the bond of reinforcement and concrete through experimental methods. The test is divided into two phases: (i) steel pulling when bonded with low-strength concrete; (ii) pulling steel out of high-strength concrete. The results provide equations to calculate bond stress and serve as a basis for further research.

E.P. Carvalho, et al. (2017) [14] studied the bonding force of strengthened concrete and smaller diameter reinforcement experimentally with different anchoring methods. The experiment shows that each steel anchor length yields different results, concluding that a specific length provides the greatest bonding ability between concrete and reinforcement.

F. Li, et al. (2013) [15] conducted experiments on the effect of corrosion on the bond between steel and concrete by mixing with chlorine and exposing to both indoor and

outdoor natural climates to estimate the actual effectiveness of corrosion. Evaluating the width of the crack in the corroded steel bar significantly affects the bonding ability of the concrete and reinforcement.

This study focuses on analysing the bond stress-slip behaviour of steel rebars inside RC structures subjected to accelerated corrosion over time through experiments and the finite element method. Finite element analysis using Ansys software was employed to accurately describe the data obtained from the experiment. The results of the experiment and FEM modelling are almost identical (less than 4.5% difference). The influence of steel rebar diameter, concrete strength, and boundary conditions are fully represented in the simulation model. The finite element analysis method proposed in this study can be fully applied to evaluate the working capacity of RC structures subjected to corrosion.

2. Process to obtain the corroded specimens by electrochemical corrosion method

The specimens were designed according to ACI 440.3R [16]. A model of the specimen is shown in Fig. 1. The information of specimens that were used to carry out the corrosion test shown in Table 1.

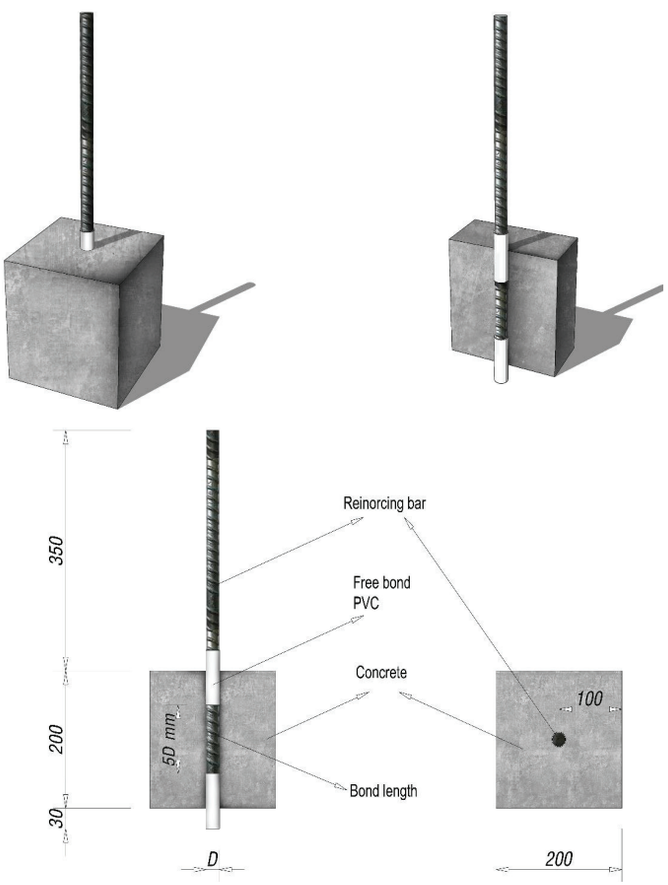

Fig. 1. Dimension and geometry of specimens.

Table 1. List of specimens were used to carry out the corrosion test.

Type of spec.	Dimension of steel bar (mm)	Bond length (mm)	Compressive strength of concrete (MPa)	Corrosion solution % NaCl	c_c (%)	M_{th} (g)	T (hour)	Number of specimens
M_{11}	12	60	25	0	0	0	0	3
M_{12}	12	60	35	0	0	0	0	3
M_{13}	12	60	45	0	0	0	0	3
M_{21}	16	80	25	0	0	0	0	3
M_{22}	16	80	35	0	0	0	0	3
M_{23}	16	80	45	0	0	0	0	3
M_{31}	20	100	25	0	0	0	0	3
M_{32}	20	100	35	0	0	0	0	3
M_{33}	20	100	45	0	0	0	0	3
$S1_{11}$-1	12	60	25	3.5	5	2.664	51.14	3
$S1_{11}$-2	12	60	25	3.5	15	7.992	153.47	3
$S1_{11}$-3	12	60	25	3.5	25	13.325	255.78	3
$S1_{12}$-1	12	60	35	3.5	5	2.664	51.14	3
$S1_{12}$-2	12	60	35	3.5	15	7.992	153.47	3
$S1_{12}$-3	12	60	35	3.5	25	13.325	255.78	3
$S1_{13}$-1	12	60	45	3.5	5	2.664	51.14	3
$S1_{13}$-2	12	60	45	3.5	15	7.992	153.47	3
$S1_{13}$-3	12	60	45	3.5	25	13.325	255.78	3
S_{21}-1	16	80	25	3.5	5	6.32	121.32	3
S_{21}-2	16	80	25	3.5	15	18.96	363.95	3
S_{21}-3	16	80	25	3.5	25	31.60	606.58	3
S_{22}-1	16	80	35	3.5	5	6.32	121.32	3
S_{22}-2	16	80	35	3.5	15	18.96	363.95	3
S_{22}-3	16	80	35	3.5	25	31.60	606.58	3
S_{23}-1	16	80	45	3.5	5	6.32	121.32	3
S_{23}-2	16	80	45	3.5	15	18.96	363.95	3
S_{23}-3	16	80	45	3.5	25	31.60	606.58	3
S_{31}-1	20	100	25	3.5	5	12.35	237.07	3
S_{31}-2	20	100	25	3.5	15	37.05	711.20	3
S_{31}-3	20	100	25	3.5	25	61.75	1,185.3	3
S_{32}-1	20	100	35	3.5	5	12.35	237.07	3
S_{32}-2	20	100	35	3.5	15	37.05	711.20	3
S_{32}-3	20	100	35	3.5	25	61.75	1,185.3	3
S_{33}-1	20	100	45	3.5	5	12.35	237.07	3
S_{33}-2	20	100	45	3.5	15	37.05	711.20	3
S_{33}-3	20	100	45	3.5	25	61.75	1,185.3	3

Three types of specimens were created to examine the effects of factors such as steel diameter, concrete strength, and corrosion duration on corrosion tests. The specimens were immersed in a 3.5% NaCl solution and then connected to the electrode system, as shown in Fig. 2. The electrode system was operated according to Faraday's law [17, 18], as shown in Table 2, with the formula presented below as:

$$M_{th} = \frac{W \times T \times I_{app}}{F} \quad (1)$$

where M_{th} is the theoretical mass of rust per unit surface area of the bar (g); W is the equivalent weight of steel, which is taken as the ratio of atomic weight of iron to the valency of iron 27.925 (g); I_{app} is the applied current density (amp); T is the duration of induced corrosion (sec); and F is Faraday's constant 96487 (amp/sec).

Fig. 2. Test samples when corrosive with salt electrolyses NaCl 3.5%.

Table 2. Electrolysis time predicted according to Faraday's law.

Dimension of rebar	Compressive strength of concrete	L (mm)	M_{th} (g)	T (hour)	c_c (%)
D12	25	60	2.664	51.14	5
	35	60	7.992	153.47	15
	45	60	13.325	255.78	25
D16	25	80	6.32	121.32	5
	35	80	18.96	363.95	15
	45	80	31.60	606.58	25
D20	25	100	12.35	237.07	5
	35	100	37.05	711.20	15
	45	100	61.75	1,185.33	25

3. Finite element method analysis programme

3.1. Finite element method bond-slip model using cohesive zone model

The FE model was established in the general FE code ANSYS 19.1. This investigation aims to simulate the bond-slip relationship; therefore, the test bar and concrete are treated separately in the model. Brick elements with 8 nodes were adopted to model the concrete, while two-node spar elements were used to model the steel reinforcements, and CZM were added to bond the nodes of the concrete and steel elements. This model is usually called a CZM because, in this model, the concrete and steel are assumed to be connected by face. It was chosen to simulate the bond-slip behaviour of concrete due to its clear mechanical principle and good connection to the experimental study. As former analyses showed that the bond behaviour of steel reinforcements inside concrete components is a 3-D nonlinear problem, the associated FE model should be able to represent the stress states and deformations in the X-, Y-, and Z-dimensions. At one position, there was a CZM connecting a pair of coincident nodes by friction force.

On the interface between the concrete and reinforcing bar, the nodes of the concrete and bars were connected by spring elements, which governed the bond-slip behaviour through their previously defined stiffness curves.

3.2. Modelling of concrete

Concrete was simulated by SOLID65, which is defined by eight nodes with three degrees of freedom at each node, that is, translation in the nodal X-, Y-, and Z-directions. The 3-D geometry and node locations of this element type are shown in Fig. 3.

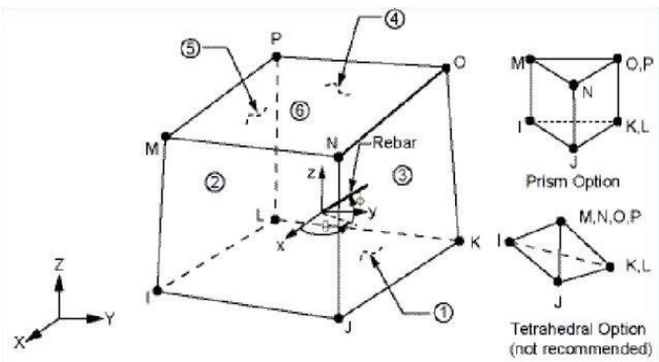

Fig. 3. SOLID65 element model.

Concrete is a quasi-brittle material that exhibits different behaviour in compression and tension. To properly model this kind of material, the SOLID65 element requires linear isotropic and multilinear isotropic material properties. The

linear isotropic properties of concrete are determined by its elastic modulus (E_c) and Poisson's ratio (υ). The compressive uniaxial stress-strain values were included to define the nonlinearities of the concrete material, meaning the stress is a nonlinear function of its strain. After yielding, ANSYS used the multilinear kinematic hardening rule to model the plastic stress-strain relationship of concrete. The elasto-plastic model with a multilinear work hardening uniaxial stress-strain curve adopted a von Mises yielding criterion (the octahedral shear stress theory). The U.S. Department of Transportation and the Federal Highway Administration (2018) [19] equivalent strains (ε_e) for the elastic and plastic

3.3. Reinforcing bar model

The reinforcing steel bars were modelled by the two-node spar element LINK180, which is an upgrade of LINK8. LINK180 is a 3-D spar element with three degrees of freedom at each node, with translations in the nodal X-, Y-, and Z-directions in Fig. 4.

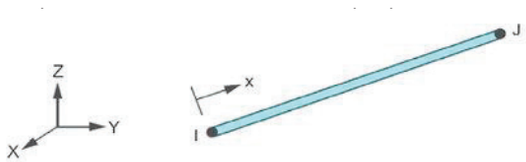

Fig. 4. LINK180 element model.

Kinematic hardening plasticity multi-linear properties are needed for reinforcements. The bilinear model requires the yield stress (f_y) and the hardening modulus of the steel (E_s). The constitutive law for steel behaviour is:

$$\begin{cases} \sigma_s = E_s\varepsilon_s, & \varepsilon_s \le 0 \\ \sigma_s = f_y + E_s'\varepsilon_s, & \varepsilon_s > \varepsilon_y \end{cases} \quad (2)$$

where σ_s is the steel stress, ε_s is the steel strain, E_s is the elastic modulus of steel, E_s' is the tangent modulus of steel after yielding, which is equal to 0.01 E_s, and f_y and ε_y are the yielding stress and strain of steel respectively.

3.4. Cohesive zone model

The CZM is used to model the interfaced bond between rebar and concrete. The main advantages of the CZM are to represent the physical properties of the interface, particularly, its fracture mechanics behaviour. The CZM response in pull-out tests and the shear cohesive stress are expressed as a function of the tangential displacement in Fig. 5. These values are identified by pull-out test experiments.

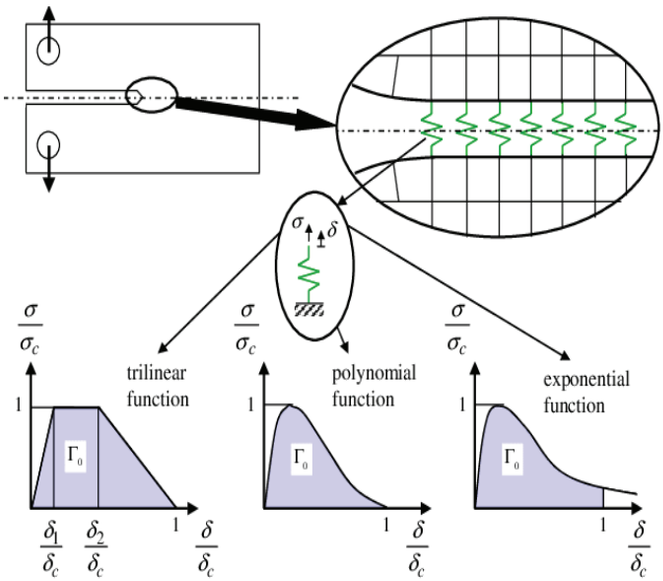

Fig. 5. Cohesive model interface behaviour between rebar and concrete.

3.5. ANSYS model

The bottom face of the concrete cube will be fixed in all directions, and a forced displacement will be applied to the top face of the rebar. This is a 3-D model, so we need to fix all degrees of freedom: UX, UY, UZ, ROTX, ROTY, and ROTZ, to prevent displacement in the horizontal and vertical directions and rotation under loading. On the other hand, applying a forced displacement will make the solution process converge more easily, as shown in Fig. 6.

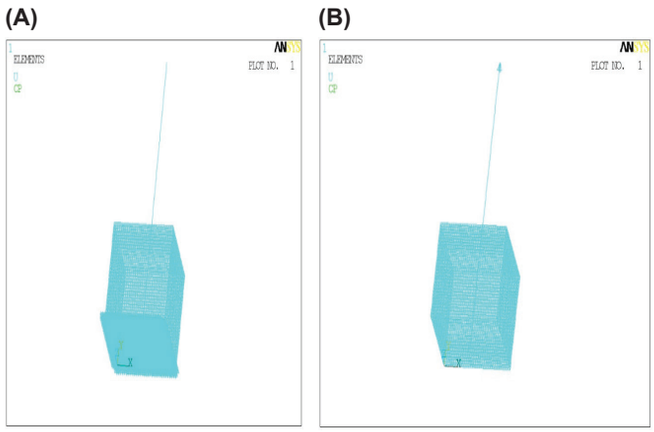

Fig. 6. (A) Boundary conditions; (B) Load conditions.

4. Results and discussion

As the rebar moves forward, tensile stress will appear in the concrete, leading to parallel cracking. All the strain and stress will concentrate at the top of the concrete specimen, as shown in Fig. 7.

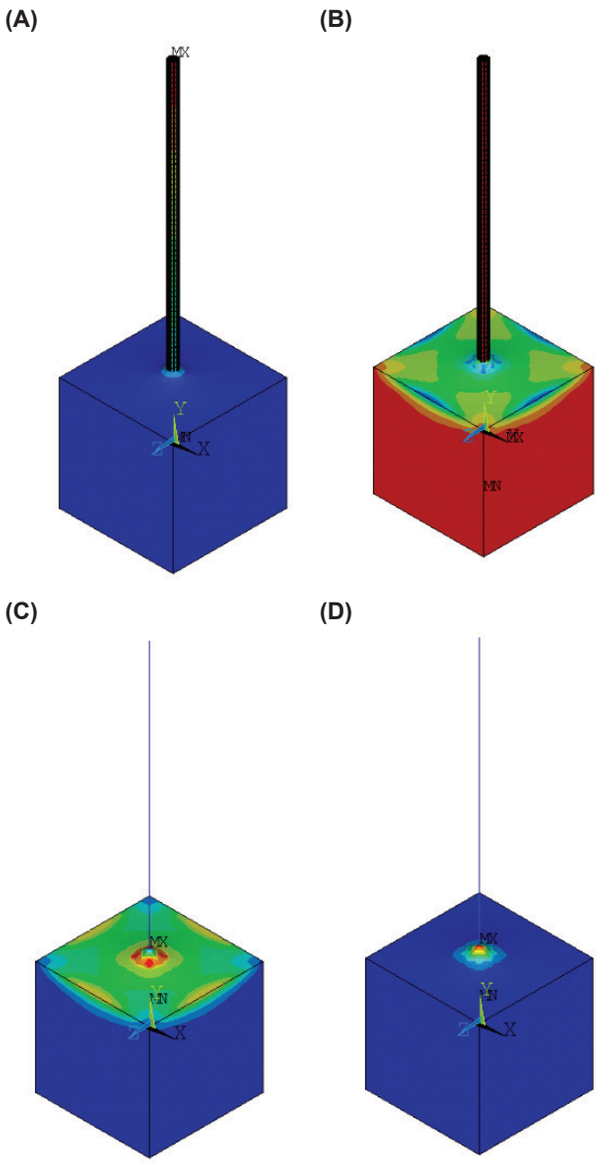

Fig. 7. (A) UY displacement; (B) Third principal stress; (C) Equivalent stress; (D) Equivalent strain.

In this process, the friction load is crucial for maintaining the connection between the rebar and the concrete.

Figures 8-16 illustrate the relationship between bond stress and slip between corroded steel bars and concrete. The diameter and compressive strength of the concrete directly affect the bond stress between the steel bars and concrete. The bond stress increases as the compressive strength increases. The average bond strength in the 24.6, 35.1, and 44.1 MPa specimens are 17.98, 22.13, and 25.88 MPa, respectively. When the steel is corroded, the bond strength is reduced. The results show that the bond stress degradation rate occurs more rapidly as the corrosion level increases and the compressive strength of the concrete increases. In a corrosive environment, the compressive strength of concrete should be no less than 35 MPa. At compressive strengths of 35.1 and 44.1 MPa, the bond strength of the steel bar and concrete will decrease by 50% when the corrosion level is about 18 and 11%, respectively. Additionally, the bearing capacity of specimens is influenced by bond stress. Therefore, with higher compressive strength, the bearing capacity of corroded RC structures deteriorates faster as the corrosion level increases. This is why the bearing capacity will increase at higher concrete strength and lower corrosion levels of the steel bar.

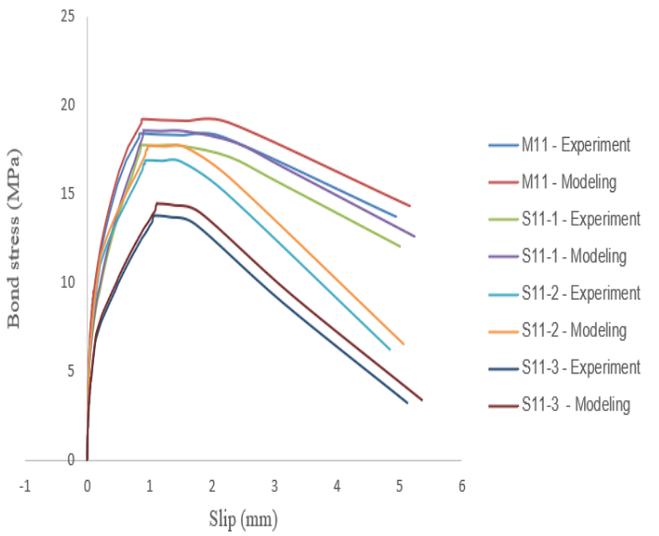

Fig. 8. The bond stress-slip relationship between experiment and finite element method of M11 group specimens.

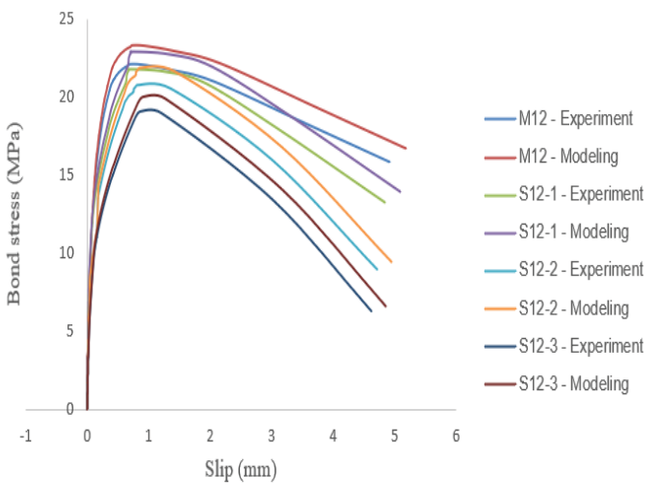

Fig. 9. The bond stress-slip relationship between experiment and finite element method of M12 group specimens.

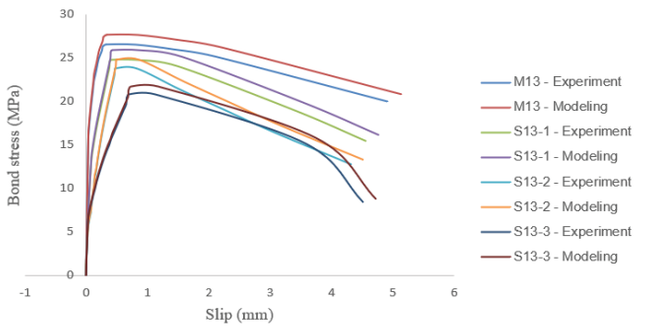

Fig. 10. The bond stress-slip relationship between experiment and finite element method of M13 group specimens.

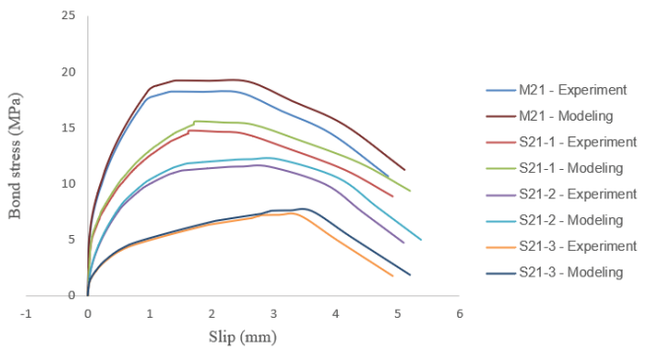

Fig. 11. The bond stress-slip relationship between experiment and finite element method of M21 group specimens.

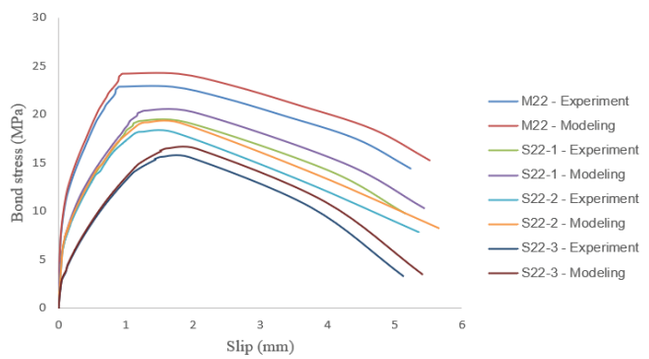

Fig. 12. The bond stress-slip relationship between experiment and finite element method of M22 group specimens.

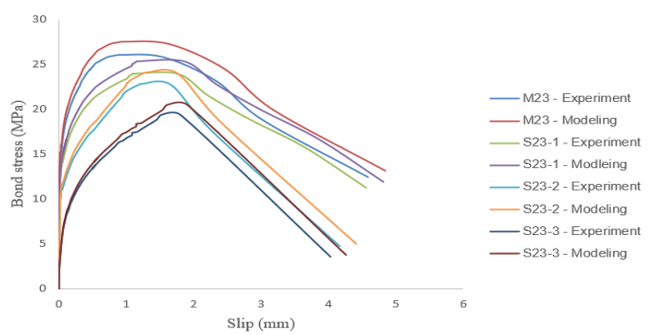

Fig. 13. The bond stress-slip relationship between experiment and finite element method of M23 group specimens.

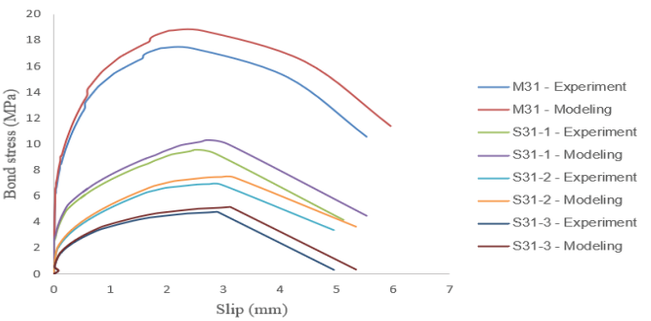

Fig. 14. The bond stress-slip relationship between experiment and finite element method of M31 group specimens.

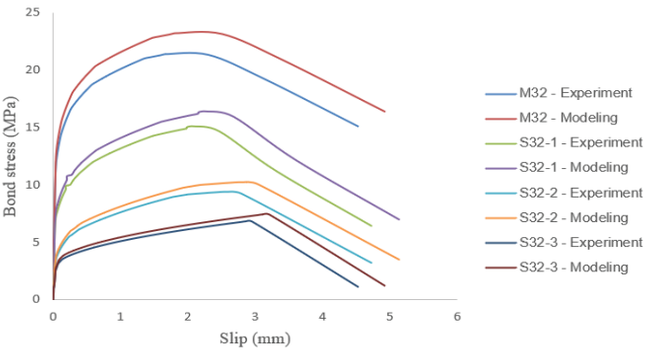

Fig. 15. The bond stress-slip relationship between experiment and finite element method of M32 group specimens.

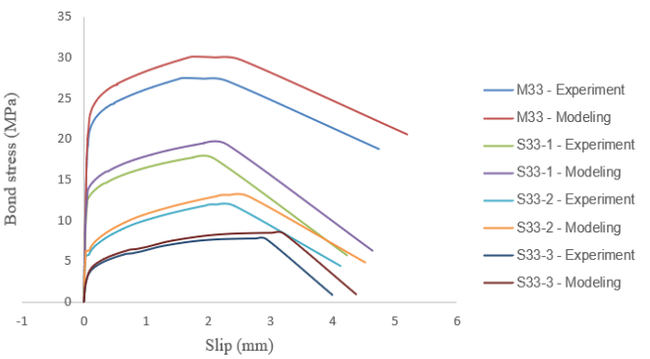

Fig. 16. The bond stress-slip relationship between experiment and finite element method of M33 group specimens.

4.1. Results of simulation of the stress-strain relationship of M1 group specimens

The results of the experiments and FEM modelling are nearly identical (less than 4.5% difference). Specifically, the first stage showed linear behaviour and second stage showed non-linear behaviour. With the value of slip being greater than 2 mm, the rebar and concrete work separately. Since the concrete grade increased, the bond stress and the slip increased as well, as shown in Figs. 8-10.

Fig. 17. Photos of (A) Cementitious matrix, (B) Steel fibres reinforcement, and (C) Mixing procedure of ultra-high performance concrete.

4.2. Results of simulation of the stress-strain relationship of M2 group specimens

In the M2 group specimens, the concrete is displaced by the rebar more than in the M1 specimens. Consequently, the discrepancy ratio between the results of the experiment and FEM modelling is larger - 5.6%. The bond stress is higher, but the slip is lower. As the grade of concrete increases, both the slip and bond stress become larger, as shown in Figs. 11-13.

4.3. Results of simulation of the stress-strain relationship of M3 group specimens

In this case, we observe that since a larger steel section has been used, the volume of concrete has decreased. The bond stress has been lower, and the slip has been higher. In summary, the connection between the rebar and the concrete is not optimal due to the increased rebar section.

In summary, using a higher grade of concrete improves its interaction with the rebar. This can help restrict structural failure, cracking, and crushing. By performing calculations and modelling to determine the optimal ratio of concrete to rebar, the best connection under loading conditions can be achieved. On the other hand, there are still differences between real testing and FEM modelling. In FEM modelling, we attempt to use the strongest material models, elements, contact conditions, and load and boundary conditions, but the results do not exactly match the testing, as shown in Figs. 14-16.

4.4. Results of simulation of bond stress in corroded and ultra-high performance concrete

Ultra-high performance concrete (UHPC) is a new class of concrete developed in recent years. The Federal Highway Administration (FHWA) defines UHPC as follows: UHPC is a cementitious composite material composed of an optimised gradation of granular constituents, a water-to-cementitious materials ratio of less than 0.25, and a high percentage of discontinuous internal fibre reinforcement. The mechanical properties of UHPC include compressive strength greater than 120 MPa and sustained post-cracking tensile strength greater than 5 MPa. Compared with conventional concrete, UHPC tends to exhibit superior properties such as advanced strength, durability, and long-term stability.

This concrete contains no coarse aggregate and is internally reinforced by 13 mm long, 0.2 mm diameter straight steel fibres included at a volumetric ratio of 2%. The UHPC mix proportions and mixing procedure are shown in Fig. 17 [20].

From the results in Fig. 18, we can observe that the bond stress increases and the slip decreases. In UHPC containing fibres and a higher grade of concrete, the rebar interacts more effectively, resulting in new specimens with UHPC performing better.

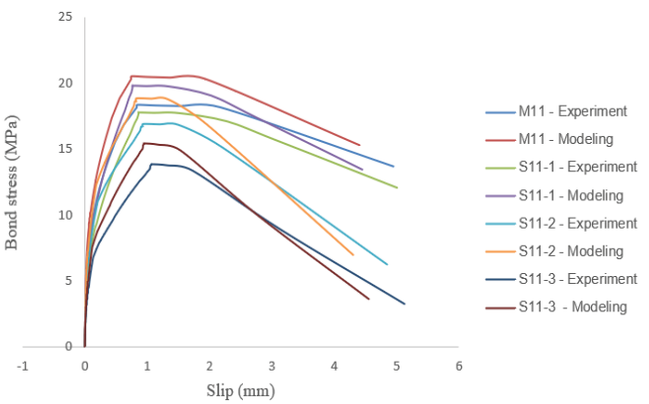

Fig. 18. The bond stress-slip relationship between experiment and finite element method of M11 group specimens with ultra-high performance concrete.

5. Conclusions

The finite element analysis method using Ansys software was applied to evaluate the bond stress-slip behaviour of steel reinforcement subjected to accelerated corrosion in conjunction with concrete. The study has yielded certain results, summarised as follows:

The experimental model was precisely constructed using Ansys software. The results obtained from finite element analysis achieved high accuracy compared to the experiment, with a maximum error of only 4.5%. The finite element method can effectively replace the experiment in analysing the adhesion force between concrete and steel.

The specimens were modelled using Ansys software. Concrete and steel rebar were modelled using the SOLID65 element and LINK180 element, respectively. The elasto-plastic behaviour for concrete and steel bars, along with the CZM for the interface bond between bars with or without corrosion and concrete, showed good agreement with experimental results. The constitutive models of materials could be applied for parametric studies in future work.

Ultra-high performance concrete was also used in experiments and finite element analysis. High-strength concrete provides better protection for steel reinforcement against corrosion. Simultaneously, the bond stress-slip between concrete and steel reinforcement also increases.

The results also showed that the reduction rate of bond strength was linear as the corrosion level increased for each compressive strength of concrete. The rate of bond strength reduction occurred more rapidly with the increase in corrosion level when the concrete compressive strength was increased. All specimens with diameters of 12 mm and 16 mm without corrosion were found to fail in pull-out failure mode. Meanwhile, all specimens with diameters of 20 and 16 mm with corrosion were found to fail in splitting failure mode. After pull-out tests, all steel bars were tested in tension again. The results showed that the higher the corrosion level, the lower the yield strength of the specimen.

CRediT author statement

Nguyen Thanh Hung, Duy Kien Dao: Literature review, Conceptualisation, Constructing hardware, Data analysis, Writing - Reviewing and Editing; Doan Dinh Thien Vuong, Le Quang Tang: Conceptualisation, Constructing hardware, Programming firmware, Testing, Image preparation, FEM modeling and analysis, Testing and Debugging.

COMPETING INTERESTS

The authors declare that there is no conflict of interest regarding the publication of this article.

REFERENCES

[1] C.D. Tien, P.V. Khoan, L.Q. Hung (2003), *Final Report of Economic - Technical Project for Anti-corrosion and Protection of Reinforced Concrete Works in Coastal Areas*, Vietnam Institute for Building Science and Technology (IBST), **11**, pp.78-88 (in Vietnamese).

[2] N.N. Thang (2006), *Application Study of Calcium Nitrite as an Additive to Inhibit Reinforcement for Reinforced Concrete in Vietnam*, Doctoral Thesis, Vietnam Institute for Building Science and Technology (IBST).

[3] A. Vichot, J.P. Ollivier (2008), *Concrete Durability: Scientific Basis for The Formulation of Environmentally Sustainable Concretes*, Presses of The National School of Bridges and Roads, 870pp (in French).

[4] Vietnam Ministry of Construction (2016), *Training Materials, Laboratory Training on Corrosion of Concrete and Steel Concrete* (Training program Project 1511).

[5] Vietnam Standards and Quality Institute (2012), *TCVN 9348:2012 - Reinforced Concrete - Determining Corrosion Activity of Reinforcing Steel - Potential Method* (in Vietnamese).

[6] P.V.D. Hoang, L.A. Thang, P.D. Thien (2017), "Experiment and simulate the pull force between geopolymer and the reinforcement", *The X National Conference on Mechanics*, **3**, pp.481-487 (in Vietnamese).

[7] S. Lim, M. Akiyama, D.M. Frangopol (2016), "Assessment of the structural performance of corrosion-affected RC members based on experimental study and probabilistic modeling", *Engineering Structures*, **127**, pp.189-205, DOI: 10.1016/j.engstruct.2016.08.040.

[8] M. Blomfors, K. Zandi, K. Lundgren (2018), "Engineering bond model for corroded reinforcement", *Engineering Structures*, **156**, pp.394-410, DOI: 10.1016/j.engstruct.2017.11.030.

[9] A.N. Kallias, M.I. Rafiq (2013), "Performance assessment of corroding RC beams using response surface methodology", *Engineering Structures*, **49**, pp.671-685, DOI: 10.1016/j.engstruct.2012.11.015.

[10] Z.H. Wang, L. Li, Y.X. Zhang, et al. (2019), "Bond-slip model considering freeze-thaw damage effect of concrete and its application", *Engineering Structures*, **201**, DOI: 10.1016/j.engstruct.2019.109831.

[11] W. Zhu, R. François, D. Coronelli, et al. (2013), "Effect of corrosion of reinforcement on the mechanical behaviour of highly corroded RC beams", *Engineering Structures*, **56**, pp.544-554, DOI: 10.1016/j.engstruct.2013.04.017.

[12] W. Zhu, R. François (2014), "Experimental investigation of the relationships between residual cross-section shapes and the ductility of corroded bars", *Construction and Building Materials*, **69**, pp.335-345, DOI: 10.1016/j.conbuildmat.2014.07.059.

[13] J.G. Dai, W.Y. Gao, J.G. Teng (2013), "Bond-slip model for FRP laminates externally bonded to concrete at elevated temperature", *Journal of Composites for Construction*, **17(2)**, pp.217-228, DOI: 10.1061/(ASCE)CC.1943-5614.0000337.

[14] E.P. Carvalho, E.G. Ferreira, J. Cunha, et al. (2017), "Experimental investigation of steel-concrete bond for thin reinforcing bars", *Latin American Journal of Solids and Structures*, **14(11)**, pp.1932-1951, DOI: 10.1590/1679-78254116.

[15] F. Li, Y. Yuan (2013), "Effects of corrosion on bond behavior between steel strand and concrete", *Construction and Building Materials*, **38**, pp.413-422, DOI: 10.1016/j.conbuildmat.2012.08.008.

[16] American Concrete Institute (2019), *Building Code Requirements for Structural Concrete (ACI 318-19)*, 628pp.

[17] P.R. Roberge (2008), *Corrosion Engineering: Principles and Practice*, McGraw Hill, 754pp.

[18] Analysis Systems (2020), https://www.ansys.com/, accessed 15 December 2020.

[19] U.S. Department of Transportation, Federal Highway Administration (2018), *Properties and Behavior of UHPC - Class Materials*, 170pp.

[20] D.H. Pham, B.D. Le, D.T. Khuc, et al. (2020), "Experiment and FEM Modeling of Bond Behaviors between pre-stressing strands and ultra-high-performance concrete", *Journal of Materials and Engineering Structures*, **7(4)**, pp.567-574.